



Article

# Satellite Image Time Series Analysis for Big Earth Observation Data

Rolf Simoes <sup>1,\*</sup> , Gilberto Camara <sup>1</sup> , Gilberto Queiroz <sup>1</sup> , Felipe Souza <sup>1</sup>, Pedro R. Andrade <sup>1</sup> , Lorena Santos <sup>1</sup> , Alexandre Carvalho <sup>2</sup> and Karine Ferreira <sup>1</sup>

- <sup>1</sup> National Institute for Space Research (INPE), Avenida dos Astronautas, 1758, Jardim da Granja, Sao Jose dos Campos, SP 12227-010, Brazil; gilberto.camara@inpe.br (G.C.); gilberto.queiroz@inpe.br (G.Q.); felipe.souza@inpe.br (F.S.); pedro.andrade@inpe.br (P.R.A.); lorena.santos@inpe.br (L.S.); karine.ferreira@inpe.br (K.F.)
- <sup>2</sup> National Institute for Applied Economics Research, SBS, Quadra 1 Bloco J, Brasília, DF 70076-900, Brazil; alexandre.ywata@ipea.gov.br
- \* Correspondence: rolf.simoes@inpe.br

**Abstract:** The development of analytical software for big Earth observation data faces several challenges. Designers need to balance between conflicting factors. Solutions that are efficient for specific hardware architectures can not be used in other environments. Packages that work on generic hardware and open standards will not have the same performance as dedicated solutions. Software that assumes that its users are computer programmers are flexible but may be difficult to learn for a wide audience. This paper describes *sits*, an open-source R package for satellite image time series analysis using machine learning. To allow experts to use satellite imagery to the fullest extent, *sits* adopts a time-first, space-later approach. It supports the complete cycle of data analysis for land classification. Its API provides a simple but powerful set of functions. The software works in different cloud computing environments. Satellite image time series are input to machine learning classifiers, and the results are post-processed using spatial smoothing. Since machine learning methods need accurate training data, *sits* includes methods for quality assessment of training samples. The software also provides methods for validation and accuracy measurement. The package thus comprises a production environment for big EO data analysis. We show that this approach produces high accuracy for land use and land cover maps through a case study in the Cerrado biome, one of the world's fast moving agricultural frontiers for the year 2018.

**Keywords:** big Earth observation data; data cubes; satellite image time series; machine learning and deep learning for remote sensing; R package



**Citation:** Simoes, R.; Camara, G.; Queiroz, G.; Souza, F.; Andrade, P.R.; Santos, L.; Carvalho, A.; Ferreira, K. Satellite Image Time Series Analysis for Big Earth Observation Data. *Remote Sens.* **2021**, *13*, 2428. <https://doi.org/10.3390/rs13132428>

Academic Editor: Pieter Kempeneers

Received: 29 April 2021

Accepted: 9 June 2021

Published: 22 June 2021

**Publisher's Note:** MDPI stays neutral with regard to jurisdictional claims in published maps and institutional affiliations.



**Copyright:** © 2021 by the authors. Licensee MDPI, Basel, Switzerland. This article is an open access article distributed under the terms and conditions of the Creative Commons Attribution (CC BY) license (<https://creativecommons.org/licenses/by/4.0/>).

## 1. Introduction

The growing demand for natural resources has caused major environmental impacts and is changing landscapes everywhere. Conversion of land cover due to human use is one of the key factors behind greenhouse gas emissions and biodiversity loss [1]. Spatial quantification of land use and land cover change allows societies to understand the extent of these impacts. Satellites are required to generate land cover products, since they provide a consistent, periodic, and globally reaching coverage of the planet's surface. Thus, satellite-based land cover products are essential to support evidence-based policies that promote sustainability.

There is currently an extensive amount of Earth observation (EO) data collected by an increasing number of satellites. Coupled with the adoption of open data policies by most spatial agencies, an unprecedented amount of satellite data is now publicly available [2]. This has brought a significant challenge for researchers and developers of geospatial technologies: how to design and build technologies that allow the Earth observation community to analyse big data sets?

The emergence of cloud computing services capable of storing and processing big EO data sets allows researchers to develop innovative methods for extracting information [3,4]. One of the relevant trends is to work with satellite image time series, which are calibrated and comparable measures of the same location on Earth at different times. These measures can come from a single sensor (e.g., MODIS) or by combining various sensors (e.g., Landsat 8 and Sentinel-2). When associated with frequent revisits, image time series can capture significant land use and land cover changes [5]. For this reason, developing methods to analyse image time series has become a relevant research area in remote sensing [6–8].

Multiyear time series of land cover attributes enable a broader view of land change. Time series capture both gradual and abrupt changes [9]. Researchers have used time series in applications such as forest disturbance [10], land change [11], ecological dynamics [12], agricultural intensification [13], and deforestation monitoring [14].

The traditional approach for change detection in remote sensing is to compare two classified images of the same place at different times and derive a transition matrix. Camara et al. [15] call this a space-first, time-later approach. The alternative is to adopt a time-first, space-later method, where all values of the time series are inputs for analysis. Each spatial location is associated with a time series. These algorithms first classify each time series individually and later apply spatial post-processing to capture neighbourhood information. Many authors argue that time-first, space-later methods are better suited to track changes continuously better than space-first, time-later approaches [8,12,15–17].

This paper describes *sits*, an open-source R package for satellite image time series analysis using machine learning that adopts a time-first, space-later approach. Its main contribution is to provide a complete workflow for land classification of big EO data sets. Users build data cubes from images in cloud providers, retrieve time series from these cubes, and can improve training data quality. Different machine learning and deep learning methods are supported. Spatial smoothing methods remove outliers from the classification. Best practice accuracy techniques ensure realistic assessments. The authors designed an expressive API that allows users to achieve good results with minimal programming effort.

The *sits* package incorporates new developments in image catalogues for cloud computing services. It also includes deep learning algorithms for image time series analysis published in recent papers and not available as R packages [8,18]. The authors developed new methods for quality control of training data [19]. Parallel processing methods specific for data cubes ensure efficient performance. Given these innovations, *sits* provides functionalities beyond existing R packages.

We organise this paper as follows. In Section 2, we review Earth observation data cubes, pointing out the challenges involved in building them. Section 3 presents the design decisions for the *sits* API and the internal components of the package. Section 4 shows a concrete example of using *sits* to perform land use and land cover classification in the Brazilian Cerrado and discusses the lessons learned. We conclude by pointing out further directions in the development of the package.

## 2. Earth Observation Data Cubes

The term Earth observation (EO) data cube is being widely used to refer to large collections of satellite images modelled as multidimensional structures to support time series analysis in an easy way to scientists [20]. There are different definitions of an EO data cube. Some authors refer to EO data cubes as organised collections of images [21] or to the software used to produce the data collection [22]. Others are more restrictive, defining data cubes as regular collections reprocessed to a common projection and a consistent timeline [20,23]. We propose a conceptual approach, following the idea of EO data cubes as geographical fields [24,25]. The essential property of a geographical field is its field function; for each location within a spatiotemporal extent, this function produces a set of values. This perspective leads to the following definitions.

**Definition 1.** A data cube is defined by a field function  $f : p \rightarrow \mathbf{v}, \forall p \in ST, \exists \mathbf{v}$ , where  $ST$  is a set of positions in space-time and  $\mathbf{v}$  is a vector of attributes without missing values.

**Definition 2.** An Earth observation data cube is a data cube whose spatiotemporal extent has a two-dimensional spatial component  $S : \mathbf{X} \times \mathbf{Y}$  where  $\forall p = (x_i, y_j) \in S$ , the point  $p$  can be referenced to a location on the surface of the Earth, and points in the spatial extent are mapped to a two-dimensional regular grid.

**Definition 3.** The temporal component of the spatiotemporal extent  $ST$  is a set of time intervals  $\mathbf{T} = t_1, \dots, t_n$  such that  $\forall (i, j, i \neq j), t_i \cap t_j = \emptyset$  and  $\forall (i, i + 1), \text{Meets}(t_i, t_{i+1})$ , where  $\text{Meets}(\cdot)$  is the temporal relation defined by Allen and Ferguson [26].

Definitions 1–3 capture the essential properties of an EO data cube: (a) there is a unique field function; (b) the spatial support is georeferenced; (c) temporal continuity is assured; and (d) all spatiotemporal locations share the same set of attributes; and (e) there are no gaps or missing values in the spatiotemporal extent (See Figure 1). Since the proposed definition is an abstract one, it can be satisfied by different concrete implementations.

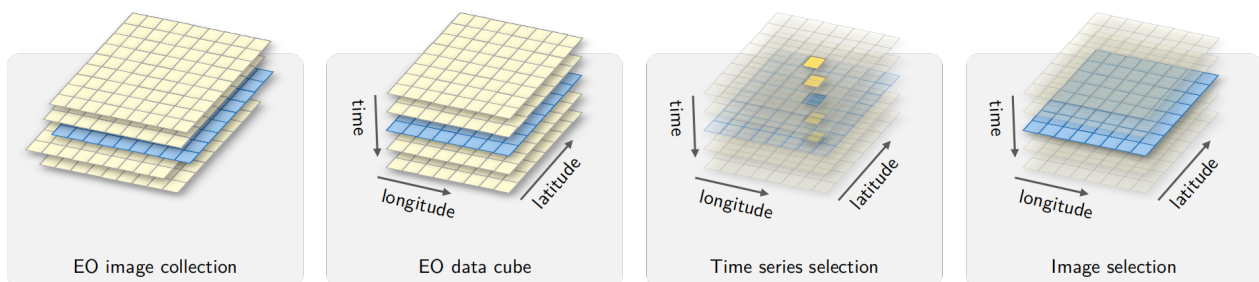


**Figure 1.** Conceptual view of data cubes (source: authors).

EO data cubes that follow these definitions enable the use of machine learning algorithms. These methods do not allow gaps or missing values in the input data. Since image collections available in cloud services do not satisfy these requirements, such collections need additional processing. This can be done either by creating a new set of files that support the properties of a data cube, or by developing software that creates data cubes in real-time. To better understand the problem, consider the differences between analysis-ready data (ARD) image collections and EO data cubes.

**Definition 4.** An ARD image collection is a set of files from a given sensor (or a combined set of sensors) that has been corrected to ensure comparable measurements between different dates. All images are reprojected to a single cartographical projection following well-established standards. Data producers usually crop ARD image collections into tiling systems.

ARD image collections do not fully support a field function, as required by Definition 1 of data cubes. These collections do not guarantee that every pixel of an image has a valid set of values since they may contain cloudy and missing pixels. For example, Figure 2 shows images of tile “20LKP” of the Sentinel-2/2A image collection available on the Amazon Web Service (AWS) for different dates. Some images have a significant number of clouds. To support the data cube abstraction, data analysis software has to replace cloudy or missing pixels with valid values.

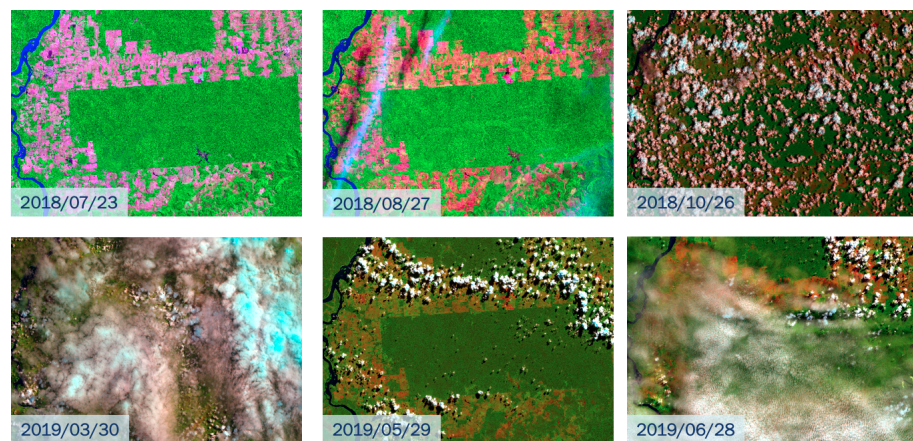


**Figure 2.** Sentinel-2 image colour composites for tile 20LKP on different dates (source: authors).

A further point concerns the timeline of different tiles. Consider the neighbouring Sentinel-2 tiles “20LLP” and “20LKP” for the period 13 July 2018 to 28 July 2019. Tile 20LLP has 144 temporal instances, while tile 20LKP has only 71 instances. Such differences in temporal extent are common in large image collections. To ensure that big areas can be processed using a single machine learning model without the need for data reprocessing, the data analysis software has to enforce a unique timeline for all tiles.

The differences between ARD image collections and data cubes proper have led some experts to develop tools that reprocess collections, making them regular in space and in time, and account for missing or noisy values. For example, the Brazil Data Cube provides organised collections [23]. The R `gdal` package supports generating consistent data cubes [20]. When designing `sits`, the authors decided that the software would support both kinds of imagery: regular data cubes and irregular image collections. The design decisions for `sits` will be further explored in the next section.

### 3. Software Design and Analysis Methods

#### 3.1. Requirements and Design Choices

The target audience for `sits` is the new generation of specialists who understand the principles of remote sensing and can write scripts in R. To allow experts to use the full extent of available satellite imagery, `sits` adopts a time-first, space-later approach. Satellite image time series are used as inputs to machine learning classifiers; the results are then post-processed using spatial smoothing. Since machine learning methods need accurate training data, `sits` includes methods for quality assessment of training samples. There are no minimum requirements for spatial or temporal extents and temporal sampling frequencies for land cover classification. The software provides tools for model validation and accuracy measurements. The package thus comprises a production environment for big EO data analysis.

We chose to develop `sits` using the R programming environment. R is well-tested and widely used for data analysis. It has high-level abstractions for spatial data, time series, and machine learning. R packages are community managed using a repository (CRAN) that enforces quality standards and cross-platform compatibility. Since `sits` is an integrated environment that supports the full cycle of land use and land cover classification, it uses a large number of third-party packages. The R CRAN community package management provides a sound basis for our work. Furthermore, the authors wanted to build robust software for big EO data analysis. Since the authors of the package include experienced R developers, the choice of R was a natural one.

Further requirements come from the authors’ affiliation with Brazil’s National Institute for Space Research (INPE). The institute provides the official Brazilian estimates of deforestation and land use change in the environmentally sensitive Amazonia and Cerrado biomes. Given the emissions and biodiversity impacts of land use change in Amazonia

and Cerrado, INPE has been providing estimates of deforestation since 1998. Since 2007, INPE also produces daily alerts of forest cuts [27]. Comprehensive assessments have shown the quality of INPE's work [28]. Since INPE experts aim to use *sits* to generate monitoring products [23], the package has been designed to meet the performance needs of operational activities.

These requirements led to the following design goals:

1. Encapsulate the land classification workflow in a concise R API.
2. Provide access to data cubes and image collections available in cloud services.
3. Develop methods for quality control of training data sets.
4. Offer a single interface to different machine learning and deep learning algorithms.
5. Support efficient processing of large areas, with internal support for parallel processing.
6. Include innovative methods for spatial post-processing.

### 3.2. Workflow and API

The design of the *sits* API considers the typical workflow for land classification using satellite image time series (see Figure 3). Users define a data cube by selecting a subset of an ARD image collection. They obtain the training data from a set of points in the data cube whose labels are known. After performing quality control on the training samples, users build a machine learning model and use it to classify the entire data cube. The results go through a spatial smoothing phase that removes outliers. Thus, *sits* supports the entire cycle of land use and land cover classification.

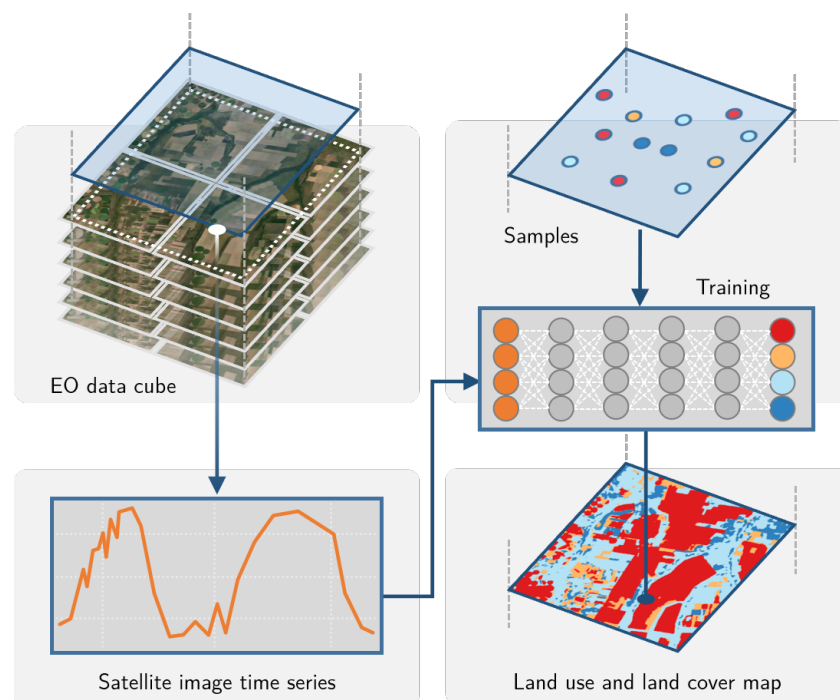


**Figure 3.** Using time series for land classification (source: authors).

The above-described workflow represents one complete cycle of land use classification. Machine learning methods require that the training data set and the classification input have the same number of dimensions. Thus, increasing or reducing the size of a data cube requires that the classification model be retrained. However, once a model has been trained, it can be applied to any data cube with the same dimensions. A model trained using samples taken from a data cube can be used for classifying another data cube, provided both cubes share the same bands and the same number of temporal intervals.

When designing the *sits* API, we tried to capture the essential properties of good software. As stated by Bloch [29], good APIs “should be easy to use and hard to misuse, and should be self-documenting”. Bloch [29] also recommends, “good programs are modular, and inter-modular boundaries define APIs”. Following this advice, in *sits*, each function carries out one task of the land classification workflow. For example, instead of having separate functions for working with machine learning models, there is one function for model training. The `sits_train()` function encapsulates all differences between different methods, ranging from random forests to convolutional neural networks. All functions have convenient default parameters. Thus, novice users can achieve good results, while more experienced ones are able to fine-tune their models to get further improvements.

The *sits* API captures the main steps of the workflow. These functions are: (a) `sits_cube()` creates a cube; (b) `sits_get_data()` extracts training data from the cube; (c) `sits_train()` trains a machine learning model; (d) `sits_classify()` classifies the cube and produces a probability cube; (e) `sits_smooth()` performs spatial smoothing using the probabilities; (f) `sits_label_classification()` produces the final labelled image. Since these functions encapsulate the core of the package, scripts in *sits* are concise and easy to reuse and reproduce.

### 3.3. Handling Data Cubes

The *sits* package works with ARD image collections available in different cloud services such as AWS, Microsoft, and Digital Earth Africa. It accepts ARD image collections as input and has user-transparent internal functions that enforce the properties of data cubes (Definitions 1–3). Currently, *sits* supports data cubes available in the following cloud services: (a) Sentinel-2/2A level 2A images in AWS and on Microsoft’s Planetary Computer; (b) collections of Sentinel, Landsat, and CBERS images in the Brazil Data Cube (BDC); (c) collections available in Digital Earth Africa; (d) data cubes produced by the `gdal.cubes` package [20]; (e) local files.

The big EO data sets available in cloud computing services are constantly being updated. For this reason, *sits* uses the STAC (SpatioTemporal Asset Catalogue) protocol. STAC is a specification of geospatial information adopted by providers of big image collections [30]. Using STAC brings important benefits to *sits*, since the software is able to access up-to-date information through STAC end-points.

Using *sits*, the user defines a data cube by selecting an ARD image collection and determining a space-time extent. Listing 1 shows the definition of a data cube using AWS Sentinel-2/2A images. The user selects the “Sentinel-2 Level 2” collection in the AWS cloud service. The data cube’s geographical area is defined by the tile “20LKP” and the temporal extent by a start and end date. Access to other cloud services works in similar ways. Data cubes in *sits* contain only metadata; access to data is done on an as-need basis.

**Listing 1.** Defining a data cube in *sits*.

---

```
s2_cube <- sits_cube(
  source      = "AWS",
  name        = "T20LKP_2018_2019",
  collection  = "sentinel-s2-l2a",
  tiles       = c("20LKP", "20LLP"),
  start_date  = "2018-07-18",
  end_date    = "2018-07-23",
  s2_resolution = 20
)
```

---

### 3.4. Handling Time Series

Following the approach taken by the `sf` R package for handling geospatial vector objects [31], *sits* stores time series in an object-relational table. As shown in Figure 4, a *sits* time series table contains data and metadata. The first six columns contain the

metadata: spatial and temporal information, the label assigned to the sample, and the data cube from where the data have been extracted. The spatial location is given in longitude and latitude coordinates for the WGS84 ellipsoid. For example, the first sample at location (−55.2, −10.8) has been labelled “Pasture”, being valid during the interval from 14 September 2013 to 29 August 2014. The `time_series` column contains the time series data for each spatiotemporal location.

```
#> # A tibble: 3 × 7
#>   longitude latitude start_date end_date   label   cube   time_series
#>   <dbl>    <dbl> <date>   <date> <chr>  <chr> <list>
#> 1   -55.2   -10.8 2013-09-14 2014-08-29 Pasture MOD13Q1 <tibble [23 × 5]>
#> 2   -57.8    -9.76 2006-09-14 2007-08-29 Pasture MOD13Q1 <tibble [23 × 5]>
#> 3   -51.9   -13.4 2014-09-14 2015-08-29 Pasture MOD13Q1 <tibble [23 × 5]>
```

**Figure 4.** Data structure for time series (source: authors).

Time series tables store training data used for land use and land cover classification. They are built in two steps. Based on field observations or by interpreting high-resolution images, experts provide samples with valid locations, labels, and dates. These samples can be provided as comma-separated text files or as shapefiles. Then, `sits` uses the expert data to retrieve the values of time series for each location from the data cube, as illustrated in Listing 2.

**Listing 2.** Extracting time series from a data cube.

```
# text file containing sample information
csv_file <- "/home/user/samples.csv"
# obtain time series
samples <- sits_get_data(
  cube = s2_cube,
  file = csv_file
)
```

### 3.5. Sample Quality Control

Experience with machine learning methods shows that the limiting factor in obtaining good results is the number and quality of training samples. Large and accurate data sets are better, no matter the algorithm used [32,33], while noisy and imperfect samples have a negative effect on classification performance [34]. Software that uses machine learning for satellite image analysis needs good methods for sample quality control.

The `sits` package provides an innovative sample quality control technique based on self-organising maps (SOM) [35,36]. SOM is a dimensionality reduction technique. High-dimensional data are mapped into two dimensions, keeping the topological relations between similar patterns [37]. The input data for quality assessment is a set of training samples, obtained as described in the “Handling Time Series” subsection above. When projecting a high-dimensional data set of training samples into a 2D self-organising map, the units of the map (called “neurons”) compete for each sample. It is expected that good quality samples of each label should be close together in the resulting map. The neighbours of each neuron of a SOM map provide information on intra-class and inter-class variability.

The function `sits_som_map()` creates a SOM to assess the quality of the samples. Each sample is assigned to a neuron based on similarity. After the samples are mapped to neurons, each neuron will be associated with a discrete probability distribution. Usually, homogeneous neurons (those with a single label) contain good quality samples. Heterogeneous neurons (those with two or more labels with significant probability) are likely

to contain noisy samples. The `sits_som_map()` function provides quality information for every sample. It also generates a 2D map that is useful to visualise class noise, since neurons associated with the same class are expected to form a cluster in the SOM map.

Figure 5 shows a SOM map for a set of training samples in the Brazilian Cerrado, obtained from the MODIS MOD13Q1 product. This set ranges from 2000 to 2017 and includes 50,160 land use and land cover samples divided into 12 labels: Dunes, Fallow–Cotton, Millet–Cotton, Soy–Corn, Soy–Cotton, Soy–Fallow, Pasture, Rocky Savanna, Savanna, Dense Woodland, Savanna Parkland, and Planted Forest. Visual inspection shows several outlier neurons located far from their label cluster. For example, while the neurons associated with the “Pasture” label form a cluster, some of those linked to the “Rocky Savanna” label are mixed among those labelled “Dense Woodland”, an unexpected situation. The quantitative evaluation confirms this intuitive insight. As shown by Santos et al. [36], removing these and other outliers improves classification results.

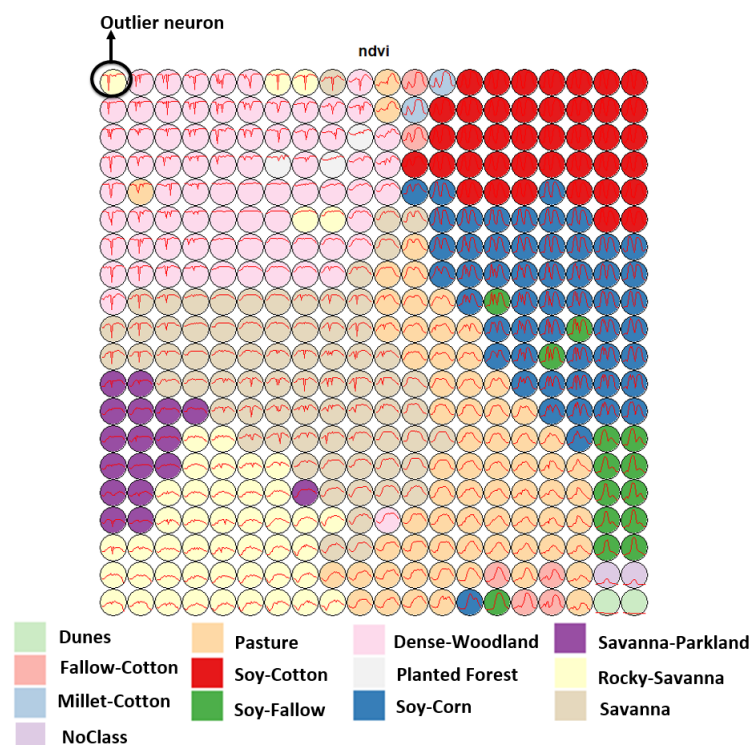


**Figure 5.** SOM map for Cerrado training samples (source: authors).

### 3.6. Training Machine Learning Models

One of the key features of machine learning and deep learning models is their dependence on the training data sets [32,38]. Selecting good quality training samples has a stronger impact on the accuracy of the classification maps than the choice of the machine learning method. For this reason, the `sits` package has been designed to support users to freely choose the training data and its labels. For each specific region of the globe and each specific aim, users select labels that match their classification schemes. Users provide samples that include geographical position, start and end dates, and a label. The package will then extract the associated time series from the data cube and use them as training data. There are no constraints on the choice of labels for the time series used for training models.

After selecting good quality samples, the next step is to train a machine learning model. The package provides support for the classification of time series, preserving the full temporal resolution of the input data. It supports two kinds of machine learning methods. The first group of methods does not explicitly consider spatial or temporal dimensions; these models treat time series as a vector in a high-dimensional feature space. From this class of models, `sits` includes random forests [39], support vector machines [40],



extreme gradient boosting [41], and multi-layer perceptrons [42]. The authors have used these methods with success for classifying large areas [23,43,44]. Our results show that, given good quality samples, *sits* can achieve high classification accuracy using feature space machine learning models.

The second group of models comprises deep learning methods designed to work with image time series. Temporal relations between observed values in a time series are taken into account. Time series classification models for satellite data include 1D convolution neural networks (1D-CNN) [8,18], recurrent neural networks (RNN) [45], and attention-based deep learning [46,47]. The *sits* package supports a set of 1D-CNN algorithms: TempCNN [8], ResNet [48], and InceptionTime [18]. Models based on 1D-CNN treat each band of an image time separately. The order of the samples in the time series is relevant for the classifier. Each layer of the network applies a convolution filter to the output of the previous layer. This cascade of convolutions captures time series features in different time scales [8]. In the Results section of the paper, we show the use of a TempCNN model to classify the Cerrado biome in Brazil for the year 2018.

Since *sits* is aimed at remote sensing users who are not machine learning experts, the package provides a set of default values for all classification models. These settings have been chosen based on extensive testing by the authors. Nevertheless, users can control all parameters for each model. The package documentation describes in detail the tuning parameters for all models that are available in the respective functions. Thus, novice users can rely on the default values, while experienced ones can fine-tune model parameters to meet their needs.

### 3.7. Data Cube Classification

The *sits* package runs in any computing environment that supports R. When working with big EO data, the target environment for *sits* is a virtual machine located close to the data repository. To achieve efficiency, *sits* implements its own parallel processing. Users are not burdened with the need to learn how to do multiprocessing and, thus, their learning curve is shortened.

Memory management in R is a hard challenge. Some advanced machine learning and deep learning methods require dedicated environments outside R. For example, deep learning methods in *sits* use the *keras* R package. In turn, this package calls Python code that provides a front-end to the C++ TensorFlow library. All of these dependencies cause R to not have a predictable memory allocation behaviour when doing parallel processing. Given this situation, we developed a customised parallel processing implementation for *sits* to work well with big EO data.

After many tests with different R packages that provide support for parallel processing, we found out that no current R package meets our needs. The authors implemented a new fault tolerant multi-tasking procedure for big EO data classification. Image classification in *sits* is done by a cluster of independent workers linked to one or more virtual machines. To avoid communication overhead, all large payloads are read and stored independently; direct interaction between the main process and the workers is kept at a minimum. The customised approach is depicted in Figure 6.

1. Based on the size of the cube, the number of cores, and the available memory, divide the cube into chunks.
2. The cube is divided into chunks along its spatial dimensions. Each chunk contains all temporal intervals.
3. Assign chunks to the worker cores. Each core processes a block and produces an output image that is a subset of the result.
4. After all the subimages are produced, join them to obtain the result.
5. If a worker fails to process a block, provide failure recovery and ensure the worker completes the job.

This approach has many advantages. It works in any virtual machine that supports R and has no dependencies on proprietary software. Processing is done in a concurrent and independent way, with no communication between workers. Failure of one worker does not cause failure of the big data processing. The software is prepared to resume classification processing from the last processed chunk, preventing against failures such as memory exhaustion, power supply interruption, or network breakdown. From an end-user point of view, all work is done smoothly and transparently.

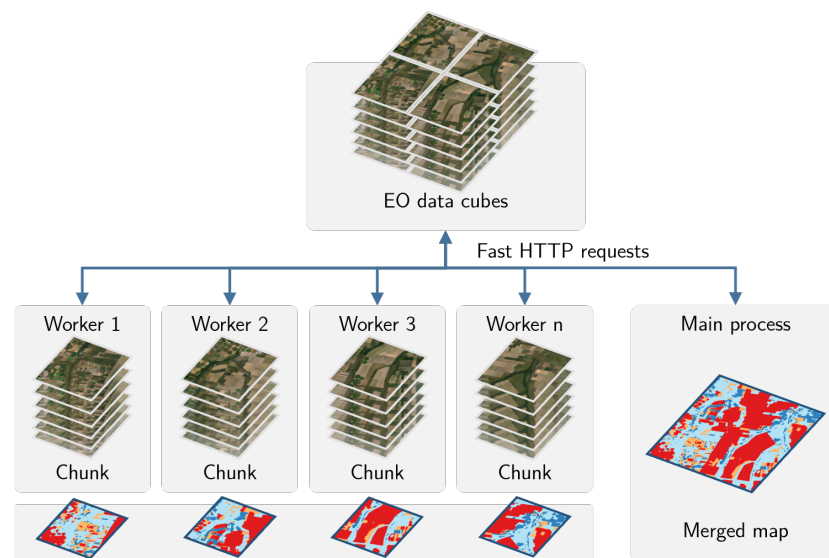


**Figure 6.** Parallel processing in sits (source: authors).

### 3.8. Post-Processing

When working with big EO data sets, there is a considerable degree of data variability in each class. As a result, some pixels will be misclassified. These errors are more likely to occur in transition areas between classes or when dealing with mixed pixels. To offset these problems, sits includes a post-processing smoothing method based on Bayesian probability that uses information from a pixel's neighbourhood to reduce uncertainty about its label.

The post-classification smoothing uses the output probabilities of a machine learning algorithm. Generally, we label a pixel  $p_i$  as being of class  $k$  if the probability of that pixel belonging to class  $k$  is higher than any other probability associated with the pixel. Instead of using these probabilities directly, Bayesian smoothing first performs a mathematical transformation by taking the log of the odds ratio for each pixel.

$$\mathbf{x}_i = \log[p_{i,k}/(1 - p_{i,k})] \quad (1)$$

To allow mathematical tractability, we assume that  $\mathbf{x}_i$  follows a multivariate normal distribution  $\mathcal{N}_k(\boldsymbol{\theta}_i, \boldsymbol{\Sigma}_i)$  where  $k$  is the number of classes. This distribution has an unknown mean  $\boldsymbol{\theta}_i$  and an estimated a priori covariance matrix  $\boldsymbol{\Sigma}_i$  that controls the level of smoothness to be applied. The covariance matrix represents our prior belief in the class variability and possible confusion between classes.

The local uncertainty is modelled by a multivariate normal distribution  $\mathcal{N}_k(\mathbf{m}_i, \mathbf{S}_i)$  where  $k$  is the number of classes. The distribution has mean  $\mathbf{m}_i$  and covariance matrix  $\mathbf{S}_i$ . Our strategy to reduce local uncertainty is to estimate these parameters from the neighbourhood of pixel  $p_i$ . Taking  $\mathbf{X}_i$  as the set of all  $\mathbf{x}_i$  vectors in a neighbourhood, we compute  $\mathbf{m}_i = E[\mathbf{X}_i]$  and  $\mathbf{S}_i = \text{cov}[\mathbf{X}_i, \mathbf{X}_i]$ . The point estimator  $\hat{\boldsymbol{\theta}}_i$  for each pixel

$p_i$  that minimises the quadratic loss functions can be obtained by applying Bayes' rule. The posterior estimator for the pixel's probabilities can be expressed as

$$\hat{\theta}_i = E[\theta_i | \mathbf{x}_i] = \Sigma_i (\Sigma_i + \mathbf{S}_i)^{-1} \mathbf{m}_i + \mathbf{S}_i (\Sigma_i + \mathbf{S}_i)^{-1} \mathbf{x}_i. \quad (2)$$

This estimator is computed for each pixel, producing a smoothed map. It is a weighted combination of  $\mathbf{x}_i$  and the neighbourhood mean  $\mathbf{m}_i$ , where the weights are determined by the covariance matrices  $\Sigma_i$  and  $\mathbf{S}_i$ . The component  $(\Sigma_i + \mathbf{S}_i)^{-1}$  plays a normalisation role. Given that the smoothing factor  $\Sigma_i$  is provided a priori by the user, the estimate depends only on the neighbourhood covariance matrix  $\mathbf{S}_i$ . When the  $\mathbf{X}$  values in a neighbourhood of a pixel are similar, the matrix  $\mathbf{S}_i$  increases relative to  $\Sigma_i$ . In this case, we will have more confidence in the original pixel value and less confidence in the neighbourhood mean  $\mathbf{m}$ . Likewise, when the  $\mathbf{X}$  values in a neighbourhood of a pixel are diverse, the values of the correlation matrix will be low. Thus, the weight expressed by  $\mathbf{S}_i$  will decrease relative to  $\Sigma_i$ . We will have less confidence in the original pixel value  $\mathbf{x}_i$  and more confidence in the local mean  $\mathbf{m}_i$ . The smoothing procedure is thus most relevant in situations where the original classification odds ratio is low, indicating a low level of separability between classes. In these cases, the updated values of the classes will be influenced by the local class variance. The resulting smoothed map will thus consider the influence of the neighbours only when the confidence in the most likely label for a pixel is low. Bayesian smoothing is an established technique for handling outliers in spatial data [49]. Its application in *sits* is useful to incorporate spatial effects in the result of time series classification.

### 3.9. Validation and Accuracy Assessment

The *sits* package offers support for cross-validation of training models and accuracy assessment of results. Cross-validation estimates the expected prediction error. It uses part of the available samples to fit the classification model, and a different part to test it. The *sits* software performs *k-fold* validation. The data are split into *k* partitions with approximately the same size. The model is tested *k* times. At each step, *sits* takes one distinct partition for testing and the remaining *k* – 1 partitions for training the model. The results are averaged to estimate the prediction error. The estimates provided by validation are a “best-case” scenario, since they only use the training samples, which are subject to selection bias. Thus, validation is best used to compare different models for the same training data. Such results must not be used as accuracy measures.

To measure the accuracy of classified images, *sits* provides a function that calculates area-weighted estimates [50,51]. The need for area-weighted estimates arises because land use and land cover classes are not evenly distributed in space. In some applications (e.g., deforestation) where the interest lies in assessing how much has changed, the area mapped as deforested is likely to be a small fraction of the total area. If users disregard the relative importance of small areas where change is taking place, the overall accuracy estimate will be inflated and unrealistic. For this reason, the `sits_accuracy_area()` function adjusts the mapped areas to eliminate bias resulting from classification error. This function provides error-adjusted area estimates with confidence intervals, following the best practices proposed by Olofsson et al. [50,51].

### 3.10. Extensibility

Since one of the design aims of *sits* is to keep a simple application programming interface, it uses the R S3 object model, which is easily extensible. The designers gave particular attention to the support required for machine learning researchers to include new models in *sits*. For machine learning models, *sits* uses two R constructs. In R, classifiers should provide a `predict` function, which carries out the actual assignment of input to class probabilities. R also provides support for closures, which are functions written by functions [52]. Using closures is particularly useful for dealing with machine learning functions that have completely different internal implementations. The `sits_train()` function in *sits* is a closure that encapsulates the details of how the classifier works.

The closure returns a function to classify time series and data cubes using the overloaded R `predict` function. Therefore, training and classification in `sits` are independent and extensible. Users can provide new models without any need for changing the other components of the package. We expect that both the authors and other contributors to the package will include further advanced models tailored for image time series.

Furthermore, `sits` can be used together with other R packages or integrated with different programming languages. It can be used to prepare time series for other algorithms, since time series in `sits` use a tabular format easily exportable to open access formats. Images associated with a data cube can also be exported from cloud providers to local repositories. Users can save deep learning classification models in TensorFlow format for later processing. Python programmers can access the full `sits` API through interface packages such as `rpy2`. This broadens the potential community of contributors and users of `sits`.

#### 4. Results and Discussion

In this section, we present an application of `sits` to produce a one-year land use and cover classification of the Cerrado biome in Brazil using Landsat-8 images. Cerrado is the second largest biome in Brazil with 1.9 million km<sup>2</sup>. The Brazilian Cerrado is a tropical savanna ecoregion with a rich ecosystem ranging from grasslands to woodlands. It is home to more than 7000 species of plants with high levels of endemism [53]. It includes three major types of natural vegetation: *Open Cerrado*, typically composed of grasses and small shrubs with a sporadic presence of small tree vegetation; *Cerrado Sensu Stricto*, a typical savanna formation, characterised by the presence of low, irregularly branched, thin-trunked trees; and *Cerradão*, a dry forest of medium-sized trees (up to 10–12 m) [54,55]. Its natural areas are being converted to agriculture at a fast pace, as it is one of the world's fast moving agricultural frontiers [56]. The main agricultural land uses include cattle ranching, crop farms, and planted forests.

##### 4.1. Input Data

The Brazilian Cerrado is covered by 51 Landsat-8 tiles available in the Brazil Data Cube (BDC) [57]. Each Landsat tile in the BDC covers a 3° × 2° grid in Albers equal area projection with an area of 73,920 km<sup>2</sup>, and a size of 11,204 × 7324 pixels. The one-year classification period ranges from September 2017 to August 2018, following the agricultural calendar. The temporal interval is 16 days, resulting in 24 images per tile. We use seven spectral bands plus two vegetation indexes (NDVI and EVI) and the cloud cover information. The total input data size is about 8 TB.

##### 4.2. Training Samples

Since the Cerrado is Brazil's main agricultural frontier, our classification aims to identify both natural vegetation and agricultural lands. Its large latitude gradient includes different climate regimes, which lead to important differences in the spectral responses of land cover types. To classify the biome with good accuracy, one needs a large and good quality sample set. To obtain good training data, we carried out a systematic sampling using a grid of 5 × 5 km throughout the Cerrado biome, collecting 85,026 samples. The training data labels were extracted from three sources: the pastureland map of 2018 from Pastagem.org [58], MapBiomas Collection 5 for 2018 [59], and Brazil's National Mapping Agency IBGE maps for 2016–2018 [60]. Out of the 85,026 samples, we selected those where there was no disagreement between the labels assigned by the three sources. The resulting set had 48,850 points from which we extracted the time series using the Landsat-8 data cube. The distribution of samples for each class is the following: "Annual Crop" (6887), "Cerradao" (4211), "Cerrado" (16,251), "Natural Non Vegetated" (38), "Open Cerrado" (5658), "Pasture" (12,894), "Perennial Crop" (68), "Silviculture" (805), "Sugarcane" (1775), and "Water" (263). The effort to obtain representative samples is justified by the importance of training data in the classification results.

### 4.3. Training and Classification

The data set of 48,850 samples was used to train a convolutional neural network model using the TempCNN method [8]. All available attributes in the BDC Landsat-8 data cube (two vegetation indices and seven spectral bands) were used for training and classification. The `sits` commands are illustrated in Listing 3. We used the default configuration of the TempCNN method with three 1D convolutional layers [8]. After the classification, we applied Bayesian smoothing to the probability maps and then generated a labelled map by selecting the most likely class for each pixel. The classification was executed on an Ubuntu server with 24 cores and 128 GB memory. Each Landsat-8 tile was classified in an average of 30 min, and the total classification took about 24 h. Figure 7 shows the final map.

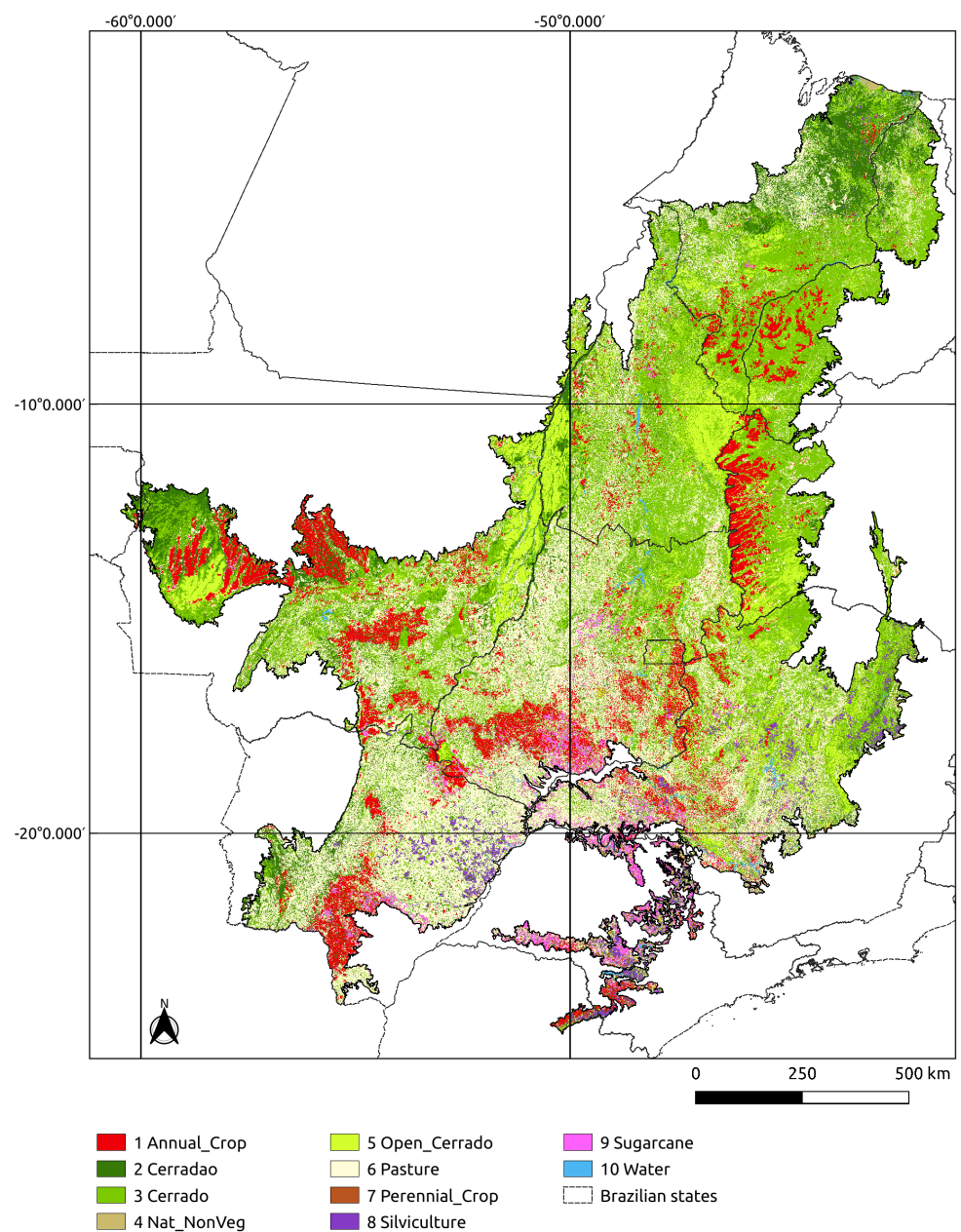


Figure 7. Cerrado land use and land cover map for 2018 (source: authors).

#### 4.4. Code

According to the principles of sits API, each function is responsible for one of the workflow tasks. As a consequence, the classification of the whole Cerrado (200 million ha) is achieved by six R commands, as shown in Listing 3.

**Listing 3.** R Code for Cerrado classification.

---

```

# define a reference to a data cube stored in the BDC using
# a shapefile with Cerrado boundaries as a region of interest
l8_cerrado_cube <- sits_cube(
  source      = "BDC",
  name        = "cerrado",
  collection  = "LC8_30_16D_STK-1",
  roi         = "./cerrado.shp",
  start_date  = "2017-09-01",
  end_date    = "2018-08-31"
)
# obtain the time series for the samples
# input data is a CSV file
samples_cerrado_lc8 <- sits_get_data(
  data = cube,
  file = "./samples_48K.csv"
)
# train model using TempCNN algorithm
cnn_model <- sits_train(
  data      = samples_cerrado_lc8,
  ml_method = sits_TempCNN()
)
# classify data cube
probs_cerrado <- sits_classify(
  data      = l8_cerrado_cube,
  ml_model  = cnn_model
)
# compute Bayesian smoothing
probs_smooth <- sits_smooth(
  data = probs_cerrado
)
# generate thematic map
map <- sits_label_classification(
  data = probs_smooth
)

```

---

#### 4.5. Classification Accuracy

To obtain an accuracy assessment of the classification, we did a systematic sampling of the Cerrado biome using a  $20 \times 20$  km grid with a total of 5402 points. These samples are independent of the training set used in the classification. They were interpreted by five specialists using high resolution images from the same period of the classification. For the assessment, we merged the labels "Cerradao", "Cerrado", and "Open Cerrado" into one label called "Cerrado". We also did additional sampling to reach a minimal number of samples for the classes "Natural Non Vegetated", "Perennial Crop", and "Water". This resulted in 5286 evaluation samples thus distributed: "Annual Crop" (553), "Cerradao" (704), "Cerrado" (2451), "Natural Non Vegetated" (44), "Pasture" (1246), "Perennial Crop" (38), "Silviculture" (94), "Sugarcane" (77), and "Water" (79). We used the sits implementation of

the area-weighted technique [50] to provide an unbiased estimator for the overall accuracy and the total area of each class based on the reference samples. The classification accuracies are shown in Table 1. The overall accuracy of the classification was 0.86.

**Table 1.** Area-weighted classification accuracy.

Labels	Producer's Accuracy	User's Accuracy
Annual Crop	0.81	0.88
Cerrado	0.89	0.91
Natural Non Vegetated	0.63	0.95
Pasture	0.82	0.76
Perennial Crop	0.51	0.74
Silviculture	0.83	0.91
Sugarcane	0.96	0.81
Water	0.93	0.97

Overall Accuracy: 0.86.

#### 4.6. Discussion of Results

The good results of mapping the entire Cerrado biome using *sits* show that the software has met its design goals. It was possible to classify a large area of about 200 million ha using an advanced deep learning model on time series with good performance. Running the whole training and classification process requires a script with only six R commands. No specific knowledge of parallel processing was required. All in all, the concept of having an integrated solution has been demonstrated.

The classes that have the worst performance are “Perennial Crop” and “Natural Non Vegetated” with producer’s accuracy of 51% and 63%, respectively. Since these classes are associated with small areas of the Cerrado biome, they had fewer training samples. The authors had access to only 68 samples of the “Perennial Crop” class and 38 samples of the “Natural Non Vegetated” class. To improve the accuracy of these classes, future classifications need to ensure that the number of samples per class is balanced and representative.

### 5. Comparative Analysis

Considering the aims and design of *sits*, it is relevant to discuss how its design and implementation choices differ from other open-source algorithms for the analysis of image time series. Such algorithms include BFAST for detecting trends and breaks [5], CCDC for continuous change detection [61], and Time-Weighted Dynamic Time Warping (TWDTW) for land use and land cover classification [62]. These methods take a multiyear time series and break it into segments, which are then classified. In general, time series segments have different temporal extents. Classified pixels will have one label for each segment of the associated time series. BFAST detects trends and seasonal components in time series and has been used successfully to detect deforestation and forest degradation [63]. CCDC decomposes the time series using spherical harmonics, extracting metrics for each segment; these metrics are used by random forest models to obtain land cover maps [64]. CCDC and BFAST are adaptive algorithms, which can be updated as new observations become available. TWDTW uses a modified version of the dynamic time warping (DTW) distance to match time series segments to predefined patterns. The TWDTW algorithm has been used for deforestation and cropland mapping [65,66]. Thus, BFAST, CCDC, and TWDTW are segmentation-based algorithms that differ in the ways to find breaks in the time series.

In contrast to segmentation-based methods, *sits* uses time series of predefined sizes for classification, typically covering one year. Instead of extracting metrics from time series segments, *sits* uses all values of the time series. There are two types of classifiers: (a) feature space methods, where all inputs are treated equally as part of an n-dimensional space, including SVM, Random Forest, and multilayer perceptrons; and (b) multiresolution methods based on 1D convolutional neural networks, including TempCNN and

ResNet [8,18]. The authors are not aware of benchmarks comparing segmentation-based methods with those based on feature space or multiresolution. As the field of satellite image time series analysis matures, users will find enough evidence to choose which method best fits their needs.

In what follows, we also compare `sits` to other approaches for big EO data analytics, such as Google Earth Engine [3], Open Data Cube [21] and openEO [67].

Google Earth Engine (GEE) [3] uses the Google distributed file system [68] and its map-reduce paradigm [69]. By combining a flexible API with an efficient back-end processing, GEE has become a widely used platform [70]. To use deep learning models in GEE, users have to develop, train and run these models outside of the Earth Engine in Google's AI platform. Since Google's AI platform does not have ready-to-use models for satellite image time series, users have to develop models for EO data analysis using the TensorFlow API. Doing so requires specialised knowledge outside of the scope of most remote sensing experts. Images also need to be exported from GEE to the AI platform, a task that can be cumbersome for large data sets. By contrast, `sits` provides support for deep learning models that have been tested and validated in the scientific literature [8,18]. These models are available directly in the `sits` API; users do not need to understand TensorFlow to apply them. Thus, currently it is easier to use `sits` than GEE for running deep learning models in image time series.

The Open Data Cube (ODC) is an important contribution to the EO community and has proven its usefulness in many domains [21,22]. It reads subsets of image collections and makes them available to users as a Python `xarray` structure. ODC does not provide an API to work with `xarrays`, relying on the tools available in Python. This choice allows much flexibility at the cost of increasing the learning curve. It also means that temporal continuity is restricted to the `xarray` memory data structure; cases where tiles from an image collection have different timelines are not handled by ODC. The design of `sits` takes a different approach, favouring a simple API with few commands to reduce the learning curve. Processing and handling large image collections in `sits` does not require knowledge of parallel programming tools. Thus, `sits` and ODC have different aims and will appeal to different classes of users.

Designers of the openEO API [67] aim to support applications that are both language-independent and server-independent. To achieve their goals, openEO designers use microservices based on REST protocols. The main abstraction of openEO is a process, defined as an operation that performs a specific task. Processes are described in JSON and can be chained in process graphs. The software relies on server-specific implementations that translate an openEO process graph into an executable script. Arguably, openEO is the most ambitious solution for reproducibility across different EO data cubes. To achieve its goals, openEO needs to overcome some challenges. Most data analysis functions are not self-contained. For example, machine learning algorithms depend on libraries such as TensorFlow and Torch. If these libraries are not available in the target environment, the user-requested process may not be executable. Thus, while the authors expect openEO to evolve into a widely used API, it is not yet feasible to base a user-driven operational software such as `sits` in openEO.

Producing software for big Earth observation data analysis requires making compromises between flexibility, interoperability, efficiency, and ease of use. GEE is constrained by the Google environment and excels at certain tasks (e.g., pixel-based processing) while being limited in others such as deep learning. ODC allows users to complete flexibility in the Python ecosystem, at the cost of limitations when working with large areas and requiring programming skills. The openEO API achieves platform independence but needs additional effort in designing drivers for specific languages and cloud services. While the `sits` API provides a simple and powerful environment for land classification, it has currently no support for other kinds of EO applications. Therefore, each of these solutions has benefits and drawbacks. Potential users need to understand the design choices and constraints to decide which software best meets their needs.



## 6. Conclusions

The development of analytical software for big EO data faces several challenges. Designers need to balance between conflicting factors. Solutions that are efficient for specific hardware architectures can not be used in other environments. Packages that work on generic hardware and open standards will not have the same performance as dedicated solutions. Software that assumes that its users are computer programmers are flexible, but may be difficult for a wide audience to learn. The challenges lead a diversity of solutions in academia and industry to work with big Earth observation data. Arguably, it is unlikely that a single approach will emerge as the complete best solution for big EO analytics.

Despite the challenges, there are points of convergence and common ground between most of the solutions for big EO data. The STAC protocol has emerged as a de facto standard for describing EO image collections. Users need interoperable and reusable solutions, where the same software can be used in different cloud services with similar results. Experience with existing solutions shows the benefits of simple APIs for the remote sensing community at large. These commonalities should be considered by big EO software designers.

In the design of *sits*, we had to make choices. We made an early choice to focus on time series analysis, based on the hypothesis that time series provide an adequate description of changes in land use and land cover. Instead of relying on time series metrics, we opted to allow machine learning methods to find patterns in multidimensional spaces by providing them all with available data. The design of the *sits* data structures and API follows from our choice of performing land classification based on time series analysis.

The limitations of *sits* should also be considered. As discussed previously, classification in *sits* uses fixed time intervals. This is a convenient choice for working with machine learning, but reduces its power to monitor continuous change. In cases where users want to monitor subtle changes such as forest degradation, segmentation-based methods can in principle provide more detailed information. Moreover, *sits* is pixel-based; each time series is associated with a pixel. Recent works show that object-based time series analysis can perform better than pixel-based approaches [66]. A further issue is the need to convert ARD image collections into data cubes to work with *sits*, as discussed in Section 2. Despite these limitations, *sits* provides a simple API for all steps of land classification using satellite image time series.

Plans for evolution of the *sits* package include improvements to the classification workflow. We plan to include manipulation of data cubes, allowing mathematical operations to be performed. Another priority is improving the training phase, using techniques such as active learning and semi-supervised learning. Moreover, we are investigating an extension of *sits* to work with spatial objects as well as including support for new classifiers. We also intend to include rule-based post-processing to allow multiyear classification comparison. Given the global applicability of *sits*, we intend to support the user and developer community by providing guidance and documentation.

**Author Contributions:** Conceptualization, G.C.; data curation, R.S.; formal analysis, R.S. and G.C.; funding acquisition, G.Q. and K.F.; investigation, R.S. and G.C.; methodology, R.S., G.C., L.S., A.C. and K.F.; resources, G.Q.; software development, R.S., G.C., G.Q., L.S., F.S. and P.R.A.; validation, R.S.; visualization, R.S., G.C., F.S. and L.S.; writing—original draft, R.S. and G.C.; writing—review and editing, G.Q., P.R.A., L.S. and K.F. All authors have read and agreed to the published version of the manuscript.

**Funding:** This research was supported by the Amazon Fund through the financial collaboration of the Brazilian Development Bank (BNDES) and the Foundation for Science, Technology and Space Applications (FUNCATE), process 17.2.0536.1. We also acknowledge support from Coordenação de Aperfeiçoamento de Pessoal de Nível Superior-Brasil (CAPES) and from the Conselho Nacional de Desenvolvimento Científico e Tecnológico (CNPq) under grant 140684/2016-6 (R.S.). Additional funding was provided by the São Paulo State Foundation (FAPESP) under eScience Program grant 2014/08398-6. This work was also supported by the International Climate Initiative of the Germany

Federal Ministry for the Environment, Nature Conservation, Building and Nuclear Safety (IKI) under grant 17-III-084- Global-A-RESTORE+ (“RESTORE+: Addressing Landscape Restoration on Degraded Land in Indonesia and Brazil”).

**Data Availability Statement:** The data and code scripts that support the findings of this study are openly available on GitHub at <https://github.com/e-sensing/sitsdata>, accessed on 14 June 2021.

**Acknowledgments:** The authors thank Marius Appel for the R package `gdalcubes` used in `sits`, Charlotte Pelletier and Hassan Fawaz for openly sharing the python code that has been reused for the TempCNN and ResNet deep learning models, and Michelle Picoli, Anderson Soares, Michel Chaves, and Alber Sánchez for collecting the validation data set.

**Conflicts of Interest:** The authors declare no conflict of interest.

**Code Availability Statement:** The `sits` package is available on Github at <https://github.com/e-sensing/sits>, accessed on 14 June 2021. The software is licensed under the GNU General Public License v3.0. Full documentation of the package is available at <https://e-sensing.github.io/sitsbook/>, accessed on 14 June 2021.

## References

- Foley, J.A.; DeFries, R.; Asner, G.P.; Barford, C.; Bonan, G.; Carpenter, S.R.; Chapin, F.S.; Coe, M.T.; Daily, G.C.; Gibbs, H.K.; et al. Global Consequences of Land Use. *Science* **2005**, *309*, 570–574. [[CrossRef](#)] [[PubMed](#)]
- Wulder, M.A.; Masek, J.G.; Cohen, W.B.; Loveland, T.R.; Woodcock, C.E. Opening the Archive: How Free Data Has Enabled the Science and Monitoring Promise of Landsat. *Remote Sens. Environ.* **2012**, *122*, 2–10. [[CrossRef](#)]
- Gorelick, N.; Hancher, M.; Dixon, M.; Ilyushchenko, S.; Thau, D.; Moore, R. Google Earth Engine: Planetary-Scale Geospatial Analysis for Everyone. *Remote Sens. Environ.* **2017**, *202*, 18–27. [[CrossRef](#)]
- Giuliani, G.; Camara, G.; Killough, B.; Minchin, S. Earth Observation Open Science: Enhancing Reproducible Science Using Data Cubes. *Data* **2019**, *4*, 147. [[CrossRef](#)]
- Verbesselt, J.; Hyndman, R.; Newnham, G.; Culvenor, D. Detecting Trend and Seasonal Changes in Satellite Image Time Series. *Remote Sens. Environ.* **2010**, *114*, 106–115. [[CrossRef](#)]
- Arvor, D.; Jonathan, M.; Meirelles, M.S.P.; Dubreuil, V.; Durieux, L. Classification of MODIS EVI Time Series for Crop Mapping in the State of Mato Grosso, Brazil. *Int. J. Remote Sens.* **2011**, *32*, 7847–7871. [[CrossRef](#)]
- Maus, V.; Camara, G.; Cartaxo, R.; Sanchez, A.; Ramos, F.M.; Queiroz, G.R. A Time-Weighted Dynamic Time Warping Method for Land-Use and Land-Cover Mapping. *IEEE J. Sel. Top. Appl. Earth Obs. Remote Sens.* **2016**, *9*, 3729–3739. [[CrossRef](#)]
- Pelletier, C.; Webb, G.I.; Petitjean, F. Temporal Convolutional Neural Network for the Classification of Satellite Image Time Series. *Remote Sens.* **2019**, *11*, 523. [[CrossRef](#)]
- Lambin, E.F.; Geist, H.J.; Lepers, E. Dynamics of Land-Use and Land-Cover Change in Tropical Regions. *Annu. Rev. Environ. Resour.* **2003**, *28*, 205–241. [[CrossRef](#)]
- Kennedy, R.E.; Yang, Z.; Cohen, W.B. Detecting Trends in Forest Disturbance and Recovery Using Yearly Landsat Time Series: 1. LandTrendr—Temporal Segmentation Algorithms. *Remote Sens. Environ.* **2010**, *114*, 2897–2910. [[CrossRef](#)]
- Zhu, Z.; Zhang, J.; Yang, Z.; Aljaddani, A.H.; Cohen, W.B.; Qiu, S.; Zhou, C. Continuous Monitoring of Land Disturbance Based on Landsat Time Series. *Remote Sens. Environ.* **2020**, *238*, 111116. [[CrossRef](#)]
- Pasquarella, V.J.; Holden, C.E.; Kaufman, L.; Woodcock, C.E. From Imagery to Ecology: Leveraging Time Series of All Available LANDSAT Observations to Map and Monitor Ecosystem State and Dynamics. *Remote Sens. Ecol. Conserv.* **2016**, *2*, 152–170. [[CrossRef](#)]
- Galford, G.L.; Mustard, J.F.; Melillo, J.; Gendrin, A.; Cerri, C.C.; Cerri, C.E. Wavelet Analysis of MODIS Time Series to Detect Expansion and Intensification of Row-Crop Agriculture in Brazil. *Remote Sens. Environ.* **2008**, *112*, 576–587. [[CrossRef](#)]
- Arvor, D.; Meirelles, M.; Dubreuil, V.; Shimabukuro, Y.E. Analyzing the Agricultural Transition in Mato Grosso, Brazil, Using Satellite-Derived Indices. *Appl. Geogr.* **2012**, *32*, 702–713. [[CrossRef](#)]
- Camara, G.; Assis, L.F.; Ribeiro, G.; Ferreira, K.R.; Llapa, E.; Vinhas, L. Big Earth Observation Data Analytics: Matching Requirements to System Architectures. In Proceedings of the 5th ACM SIGSPATIAL International Workshop on Analytics for Big Geospatial Data, San Francisco, CA, USA, 31 October 2016; ACM: Burlingame, CA, USA, 2016; pp. 1–6.
- Sudmanns, M.; Tiede, D.; Lang, S.; Baraldi, A. Semantic and Syntactic Interoperability in Online Processing of Big Earth Observation Data. *Int. J. Digit. Earth* **2018**, *11*, 95–112. [[CrossRef](#)] [[PubMed](#)]
- Woodcock, C.E.; Loveland, T.R.; Herold, M.; Bauer, M.E. Transitioning from Change Detection to Monitoring with Remote Sensing: A Paradigm Shift. *Remote Sens. Environ.* **2020**, *238*, 111558. [[CrossRef](#)]
- Fawaz, H.; Lucas, B.; Forestier, G.; Pelletier, C.; Schmidt, D.F.; Weber, J.; Webb, G.I.; Idoumghar, L.; Muller, P.A.; Petitjean, F. InceptionTime: Finding AlexNet for Time Series Classification. *Data Min. Knowl. Discov.* **2020**, *34*, 1936–1962. [[CrossRef](#)]
- Santos, L.A.; Ferreira, K.R.; Camara, G.; Picoli, M.C.A.; Simoes, R.E. Quality Control and Class Noise Reduction of Satellite Image Time Series. *ISPRS J. Photogramm. Remote Sens.* **2021**, *177*, 75–88. [[CrossRef](#)]

20. Appel, M.; Pebesma, E. On-Demand Processing of Data Cubes from Satellite Image Collections with the Gdalcubes Library. *Data* **2019**, *4*, 92. [CrossRef]
21. Lewis, A.; Oliver, S.; Lymburner, L.; Evans, B.; Wyborn, L.; Mueller, N.; Raevksi, G.; Hooke, J.; Woodcock, R.; Sixsmith, J.; et al. The Australian Geoscience Data Cube—Foundations and Lessons Learned. *Remote Sens. Environ.* **2017**, *202*, 276–292. [CrossRef]
22. Giuliani, G.; Chatenoux, B.; Piller, T.; Moser, F.; Lacroix, P. Data Cube on Demand (DCoD): Generating an Earth Observation Data Cube Anywhere in the World. *Int. J. Appl. Earth Obs. Geoinf.* **2020**, *87*, 102035. [CrossRef]
23. Ferreira, K.R.; Queiroz, G.R.; Vinhas, L.; Marujo, R.F.B.; Simoes, R.E.O.; Picoli, M.C.A.; Camara, G.; Cartaxo, R.; Gomes, V.C.F.; Santos, L.A.; et al. Earth Observation Data Cubes for Brazil: Requirements, Methodology and Products. *Remote Sens.* **2020**, *12*, 4033. [CrossRef]
24. Galton, A. Fields and Objects in Space, Time, and Space-Time. *Spat. Cogn. Comput.* **2004**, *4*, 39–68. [CrossRef]
25. Camara, G.; Egenhofer, M.J.; Ferreira, K.; Andrade, P.; Queiroz, G.; Sanchez, A.; Jones, J.; Vinhas, L. Fields as a Generic Data Type for Big Spatial Data. In *Geographic Information Science*; Springer: Berlin/Heidelberg, Germany, 2014; Volume 8728, pp. 159–172. [CrossRef]
26. Allen, J.; Ferguson, G. Actions and Events in Interval Temporal Logic. *J. Log. Comput.* **1994**, *4*, 531–579. [CrossRef]
27. Shimabukuro, Y.E.; Santos, J.R.; Formaggio, A.R.; Duarte, V.; Rudorff, B.F.T. The Brazilian Amazon Monitoring Program: PRODES and DETER Projects. In *Global Forest Monitoring from Earth Observation*; CRC Press: London, UK, 2017; p. 354.
28. Parente, L.; Nogueira, S.; Baumann, L.; Almeida, C.; Maurano, L.; Affonso, A.G.; Ferreira, L. Quality Assessment of the PRODES Cerrado Deforestation Data. *Remote Sens. Appl. Soc. Environ.* **2021**, *21*, 100444. [CrossRef]
29. Bloch, J. How to Design a Good API and Why It Matters. In *Proceedings of the 21st ACM SIGPLAN Symposium on Object-Oriented Programming Systems, Languages, and Applications*; ACM: Chicago, IL, USA, 2006; pp. 506–507. [CrossRef]
30. Hanson, M. The Open-Source Software Ecosystem for Leveraging Public Datasets in Spatio-Temporal Asset Catalogs (STAC). *AGU Fall Meet. Abstr.* 2019; p. IN23B–07. Available online: <https://ui.adsabs.harvard.edu/abs/2019AGUFMIN23B..07H/abstract> (accessed on 14 June 2021).
31. Pebesma, E. Simple Features for R: Standardized Support for Spatial Vector Data. *R J.* **2018**, *10*, 439. [CrossRef]
32. Maxwell, A.E.; Warner, T.A.; Fang, F. Implementation of Machine-Learning Classification in Remote Sensing: An Applied Review. *Int. J. Remote Sens.* **2018**, *39*, 2784–2817. [CrossRef]
33. Thanh Noi, P.; Kappas, M. Comparison of Random Forest, k-Nearest Neighbor, and Support Vector Machine Classifiers for Land Cover Classification Using Sentinel-2 Imagery. *Sensors* **2018**, *18*, 18. [CrossRef]
34. Frenay, B.; Verleysen, M. Classification in the Presence of Label Noise: A Survey. *IEEE Trans. Neural Netw. Learn. Syst.* **2014**, *25*, 845–869. [CrossRef] [PubMed]
35. Santos, L.; Ferreira, K.; Picoli, M.; Camara, G. Self-Organizing Maps in Earth Observation Data Cubes Analysis. In *Advances in Self-Organizing Maps, Learning Vector Quantization, Clustering and Data Visualization*; Vellido, A., Gibert, K., Angulo, C., Martin, J., Eds.; Springer International Publishing: Berlin/Heidelberg, Germany, 2019; pp. 70–79.
36. Santos, L.A.; Ferreira, K.; Picoli, M.; Camara, G.; Zurita-Milla, R.; Augustijn, E.W. Identifying Spatiotemporal Patterns in Land Use and Cover Samples from Satellite Image Time Series. *Remote Sens.* **2021**, *13*, 974. [CrossRef]
37. Kohonen, T. The Self-Organizing Map. *Proc. IEEE* **1990**, *78*, 1464–1480. [CrossRef]
38. Ma, L.; Liu, Y.; Zhang, X.; Ye, Y.; Yin, G.; Johnson, B.A. Deep Learning in Remote Sensing Applications: A Meta-Analysis and Review. *ISPRS J. Photogramm. Remote Sens.* **2019**, *152*, 166–177. [CrossRef]
39. Belgiu, M.; Dragut, L. Random Forest in Remote Sensing: A Review of Applications and Future Directions. *ISPRS J. Photogramm. Remote Sens.* **2016**, *114*, 24–31. [CrossRef]
40. Mountrakis, G.; Im, J.; Ogole, C. Support Vector Machines in Remote Sensing: A Review. *ISPRS J. Photogramm. Remote Sens.* **2011**, *66*, 247–259. [CrossRef]
41. Chen, T.; Guestrin, C. XGBoost: A Scalable Tree Boosting System. In *Proceedings of the 22nd ACM SIGKDD International Conference on Knowledge Discovery and Data Mining*; ACM: San Francisco, CA, USA, 2016; pp. 785–794. [CrossRef]
42. Parente, L.; Taquary, E.; Silva, A.P.; Souza, C.; Ferreira, L. Next Generation Mapping: Combining Deep Learning, Cloud Computing, and Big Remote Sensing Data. *Remote Sens.* **2019**, *11*, 2881. [CrossRef]
43. Picoli, M.; Camara, G.; Sanches, I.; Simoes, R.; Carvalho, A.; Maciel, A.; Coutinho, A.; Esquerdo, J.; Antunes, J.; Begotti, R.A.; et al. Big Earth Observation Time Series Analysis for Monitoring Brazilian Agriculture. *ISPRS J. Photogramm. Remote Sens.* **2018**, *145*, 328–339. [CrossRef]
44. Picoli, M.C.A.; Simoes, R.; Chaves, M.; Santos, L.A.; Sanchez, A.; Soares, A.; Sanches, I.D.; Ferreira, K.R.; Queiroz, G.R. CBERS Data Cube: A Powerful Technology for Mapping and Monitoring Brazilian Biomes. In *ISPRS Annals of the Photogrammetry, Remote Sensing and Spatial Information Sciences*; Nice, France, 2020; Volume V-3-2020, pp. 533–539. Available online: <https://www.isprs-ann-photogramm-remote-sens-spatial-inf-sci.net/V-3-2020/> (accessed on 14 June 2021).
45. Russwurm, M.; Korner, M. Multi-Temporal Land Cover Classification with Sequential Recurrent Encoders. *ISPRS Int. J. Geo-Inf.* **2018**, *7*, 129. [CrossRef]
46. Garnot, V.; Landrieu, L.; Giordano, S.; Chehata, N. Satellite Image Time Series Classification with Pixel-Set Encoders and Temporal Self-Attention. In *Proceedings of the 2020 IEEE/CVF Conference on Computer Vision and Pattern Recognition (CVPR)*, Seattle, WA, USA, 14–19 June 2020; IEEE: Seattle, WA, USA, 2020; pp. 12322–12331. [CrossRef]

47. Rußwurm, M.; Pelletier, C.; Zollner, M.; Lefèvre, S.; Körner, M. BreizhCrops: A Time Series Dataset for Crop Type Mapping. *arXiv* **2020**, arXiv:1905.11893
48. Fawaz, H.I.; Forestier, G.; Weber, J.; Idoumghar, L.; Muller, P.A. Deep Learning for Time Series Classification: A Review. *Data Min. Knowl. Discov.* **2019**, *33*, 917–963. [[CrossRef](#)]
49. Cressie, N. Bayesian Smoothing of Rates in Small Geographic Areas. *J. Reg. Sci.* **1995**, *35*, 659–673. [[CrossRef](#)]
50. Olofsson, P.; Foody, G.M.; Stehman, S.V.; Woodcock, C.E. Making Better Use of Accuracy Data in Land Change Studies: Estimating Accuracy and Area and Quantifying Uncertainty Using Stratified Estimation. *Remote Sens. Environ.* **2013**, *129*, 122–131. [[CrossRef](#)]
51. Olofsson, P.; Foody, G.M.; Herold, M.; Stehman, S.V.; Woodcock, C.E.; Wulder, M.A. Good Practices for Estimating Area and Assessing Accuracy of Land Change. *Remote Sens. Environ.* **2014**, *148*, 42–57. [[CrossRef](#)]
52. Wickham, H. *Advanced R*, 2nd ed.; Chapman and Hall/CRC: Boca Raton, FL, USA, 2019.
53. Klink, C.; Machado, R. Conservation of the Brazilian Cerrado. *Conserv. Biol.* **2005**, *19*, 707–713. [[CrossRef](#)]
54. Goodland, R. A Physiognomic Analysis of the ‘Cerrado’ Vegetation of Central Brasil. *J. Ecol.* **1971**, *59*, 411. [[CrossRef](#)]
55. Del-Claro, K.; Torezan-Silingardi, H.M. The Study of Biotic Interactions in the Brazilian Cerrado as a Path to the Conservation of Biodiversity. *An. Acad. Bras. Ciências* **2019**, *91*, e20180768. [[CrossRef](#)]
56. Walter, B.M.T. Fitofisionomias do Bioma Cerrado: Síntese Terminológica e relações florísticas. Ph.D. Dissertation, Universidade de Brasília, Brasília, DF, Brazil, 2006.
57. Ferreira, K.; Queiroz, G.; Camara, G.; Souza, R.; Vinhas, L.; Marujo, R.; Simoes, R.; Noronha, C.; Costa, R.; Arcanjo, J.; et al. Using Remote Sensing Images and Cloud Services on AWS to Improve Land Use and Cover Monitoring. In Proceedings of the LAGIRS 2020: 2020 Latin American GRSS & ISPRS Remote Sensing Conference, Santiago, Chile, 22–26 March 2020.
58. Parente, L.; Mesquita, V.; Miziara, F.; Baumann, L.; Ferreira, L. Assessing the Pasturelands and Livestock Dynamics in Brazil, from 1985 to 2017: A Novel Approach Based on High Spatial Resolution Imagery and Google Earth Engine Cloud Computing. *Remote Sens. Environ.* **2019**, *232*, 111301. [[CrossRef](#)]
59. Souza, C.M.; Shimbo, J.Z.; Rosa, M.R.; Parente, L.L.; Alencar, A.A.; Rudorff, B.F.T.; Hasenack, H.; Matsumoto, M.; Ferreira, L.G.; Souza-Filho, P.W.M.; et al. Reconstructing Three Decades of Land Use and Land Cover Changes in Brazilian Biomes with Landsat Archive and Earth Engine. *Remote Sens.* **2020**, *12*, 2735. [[CrossRef](#)]
60. IBGE. *Monitoramento da Cobertura e uso da Terra do Brasil: 2016–2018*; Book 101703; Brazilian Institute of Geography and Statistics: Rio de Janeiro, Brazil, 2020.
61. Zhu, Z.; Woodcock, C.E. Continuous Change Detection and Classification of Land Cover Using All Available Landsat Data. *Remote Sens. Environ.* **2014**, *144*, 152–171. [[CrossRef](#)]
62. Maus, V.; Câmara, G.; Appel, M.; Pebesma, E. dtwSat: Time-Weighted Dynamic Time Warping for Satellite Image Time Series Analysis in R. *J. Stat. Softw.* **2019**, *88*, 1–31. [[CrossRef](#)]
63. Hamunyela, E.; Verbesselt, J.; Herold, M. Using Spatial Context to Improve Early Detection of Deforestation from Landsat Time Series. *Remote Sens. Environ.* **2016**, *172*, 126–138. [[CrossRef](#)]
64. Arévalo, P.; Bullock, E.L.; Woodcock, C.E.; Olofsson, P. A Suite of Tools for Continuous Land Change Monitoring in Google Earth Engine. *Front. Clim.* **2020**, *2*. [[CrossRef](#)]
65. Cheng, K.; Wang, J. Forest-Type Classification Using Time-Weighted Dynamic Time Warping Analysis in Mountain Areas: A Case Study in Southern China. *Forests* **2019**, *10*, 1040. [[CrossRef](#)]
66. Belgiu, M.; Csillik, O. Sentinel-2 Cropland Mapping Using Pixel-Based and Object-Based Time-Weighted Dynamic Time Warping Analysis. *Remote Sens. Environ.* **2018**, *204*, 509–523. [[CrossRef](#)]
67. Schramm, M.; Pebesma, E.; Milenković, M.; Foresta, L.; Dries, J.; Jacob, A.; Wagner, W.; Mohr, M.; Neteler, M.; Kadunc, M.; et al. The openEO API—Harmonising the Use of Earth Observation Cloud Services Using Virtual Data Cube Functionalities. *Remote Sens.* **2021**, *13*, 1125. [[CrossRef](#)]
68. Ghemawat, S.; Gobioff, H.; Leung, S.T. The Google File System. In Proceedings of the Nineteenth ACM Symposium on Operating Systems Principles, Bolton Landing, NY, USA, 19–22 October 2003; ACM: Bolton Landing, NY, USA, 2003; pp. 29–43. [[CrossRef](#)]
69. Dean, J.; Ghemawat, S. MapReduce: Simplified Data Processing on Large Clusters. *Commun. ACM* **2008**, *51*, 107–113. [[CrossRef](#)]
70. Amani, M.; Ghorbanian, A.; Ahmadi, S.A.; Kakooei, M.; Moghimi, A.; Mirmazloumi, S.M.; Moghaddam, S.H.A.; Mahdavi, S.; Ghahremanloo, M.; Parsian, S.; et al. Google Earth Engine Cloud Computing Platform for Remote Sensing Big Data Applications: A Comprehensive Review. *IEEE J. Sel. Top. Appl. Earth Obs. Remote Sens.* **2020**, *13*, 5326–5350. [[CrossRef](#)]